2013 IEEE/RSJ International Conference on
Intelligent Robots and Systems (IROS)
November 3-7, 2013. Tokyo, Japan

Appropriate Biomechanics and kinematics Modeling of the respiratory System: Human Diaphragm and Thorax

Hamid Ladjal[1,2], Behzad Shariat[1], Joseph Azencot[1], Michael Beuve[2]

Abstract— **Tumor motion during irradiation reduces target coverage and increases dose to healthy tissues. Prediction of respiratory motion has the potential to substantially improve cancer radiation therapy. The respiratory motion is complex and its prediction is not a simple task, especially that breathing is controlled by the independent action of the diaphragm muscles and thorax. The diaphragm is the principal muscle used in the process of respiration and its modeling is essential for assessing the respiratory motion. In this context, an accurate patient-specific Finite Element (FE) based biomechanical model can be used to predict diaphragm deformation. In this paper, we have developed a FE model of the respiratory system including the diaphragm behavior and the complete thorax with musculoskeletal structure. These incorporate the ribs kinematics extracted directly from the Computed Tomography (CT) scan images. In order to demonstrate the effectiveness of our biomechanical model, a qualitative and quantitative comparison between the FE simulations and the CT scan images were performed. Upon application of linear elastic models, our results show that a linear elastic model can accurately predict diaphragm deformations. These comparisons demonstrate the effectiveness of the proposed physically-based model. The developed computational model could be a valuable tool for respiratory system deformation prediction in order to be controlled and monitored by external sensors during the treatment .**

I. INTRODUCTION

Prediction of respiratory motion has the potential to substantially improve cancer radiation therapy. The respiratory motion modifies both the internal organs shape and the position. This could impact negatively the quality of radiation treatment of cancer. Concerning the lung cancer, respiratory tumor motion tracking has become one of the most difficult challenge for different treatment modalities, as External Beam Radiation Therapy (EBRT)[1], Intensity Modulated Radio Therapy (IMRT)[2],[3], Stereotactic Radiation Therapy (SRT) [4] and Proton Beam Therapy (PBT) [5]. Different techniques based on imaging, such as Cone-Beam or deformable image registration, attempt to predict the position of lung tumors [6]. There are two types of image registration, rigid and deformable. Rigid registration is not suitable for organs with large deformation, such as lungs. The deformable image registration techniques have been used including intensity-based and biomechanical models. Other authors developed a method to compensate 3D non-rigid motion of soft tissue structures in the presence of respiration using 4D ultrasound [7]. However, the respiratory motion is complex and its prediction is not a simple task, especially that breathing is controlled by the independent action of the thorax and diaphragm muscles. The diaphragm moves down during the inhalation, creating negative pressure around the thoracic cavity and decreasing pressure on abdominal organs. It moves up during the exhalation, the pressure increases on the lungs and on abdominal organs (Fig.1). Consequently, the respiratory motion is non reproductible. Therefore, image based techniques could give unsatisfactory results. Therefore, we proposed a new global methodology (Fig.2) based on biomechanical modeling of the respiratory system to be used in the future to accurately predict tumour position during radiotherapy, allowing to:

- take the non-reproducible aspects of the motion into account
- establish the biomechanical model from patients geometrical and physical data
- be monitored by external sensors during the treatment
- finally, the rib kinematics method is expected to compensate the difference in biomechanical parameters from one patient to another

Therefore, some authors proposed physically based techniques to simulate respiratory organes motion. Various models have been proposed for diaphragm modeling. In this order, the main approaches are the Finite Element Method (FEM) [8], [10], Mass-Spring Models (MSMs) and chainMail [8],[9]. Generally, the MSMs are used more frequently in computer graphics for real time applications [11],[12]. However, the main drawback of these models is the lack of precision due to the difficulty of the integration of the biomechanical parameters in these models. On the

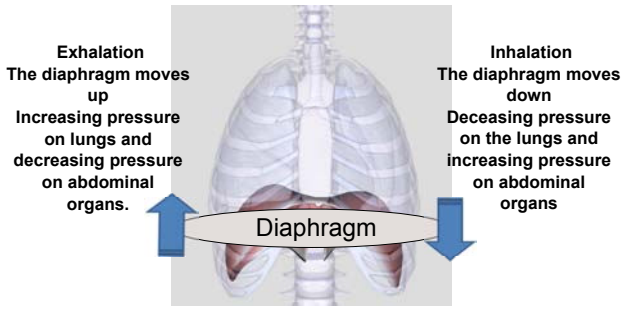

Fig. 1. Diaphragm's role in breathing: changes in the position of the diaphragm and thoracic cage during respiration.

This research is supported by the ENVISION project (co-funded by the European Commission under the FP7 Collaborative Projects Grant Agreement Nr. 241851FP7), and by ETOILE's Research Program (PRRH/UCBL, under CPER 2007-13 funding)

[1]H. Ladjal, J. Azencot, B. Shariat are with LIRIS CNRS UMR 5205, Université Claude Bernard Lyon 1, France,

[2]H. Ladjal and M. Beuve are with IPNL CNRS UMR 5822, F-69622, Université Claude Bernard Lyon 1, France. hamid.ladjal@liris.cnrs.fr

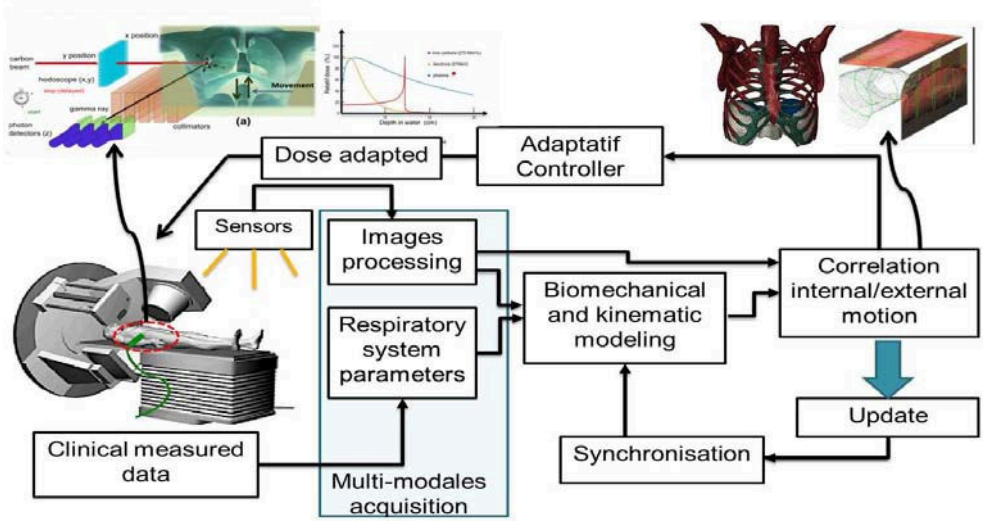

Fig. 2. Our global methodology: External surrogates and sensors track internal organs motion based an accurate patient-specific finite element (FE) based biomechanical model during treatment.

other hand, the FEM is by far the most common numerical discretization and solution technique that has been used in computational biomechanics. Biomechanical model based on finite element analysis is one of the methods proposed for predicting diaphragm deformations [10], [14].

A complex finite element patient specific model can be developed using current medical imaging modalities (such as CT or Magnetic resonance imaging MRI). In [13], the authors have proposed a numerical model including the global deformation of the diaphragm based on the HUman MOdel for Safety (HUMOS). The model is based on a linear function of muscle contraction (excitation). Unfortunately, the authors do not elaborate the mechanical behavior of the diaphragm. Other authors, have proposed an incompressible transversely isotropic hyperelastic model [14]. Their geometric model is obtained by the segmentation of the diaphragm (old female cadaver). Unfortunately, the behavior obtained from this model is not confronted with clinical data, and the influence of the rib cage are not taken in consideration.

In order to predict the internal motion caused by the respiration, we have developed a biomechanical model of the respiratory system, based on anatomical and physiological knowledge. The model includes the human diaphragm (including the tendon and muscles shape and dimensions) and the complete thorax with musculoskeletal structure (ribs, thoracic vertebra, cartilage costal margin, body of sternum) the ribcage's kinematics model, extracted directly from CT scan images. Motions and deformations are computed with the Finite Element Method (FEM). This method provide a better insight into the mechanical behavior of the organs and responses since it is based on the biomechanical properties of the material, complex organ geometry, and anatomical boundary conditions[19].

In our previous work, we have proposed a preliminary study of the respiratory system using a "virtual patient", including a simple homogenous model of the diaphragm [19]. This feasibility study is achieved without any comparison with clinical data. In [20], we have proposed a 3D biomechanical modeling of the human diaphragm based on finite element method. Unfortunately, the influence of the rib cage is not taken in consideration.

The novel aspect of our study is to show that by accurately modeling anatomical details in 3D, a linear elastic finite element model can predict diaphragm deformation. Furthermore, the results of our study show that the combinaison of rib kinematics and FE analysis can be used to develop an accurate 3D predict specific biomechanical model. Our model permits the control of simulated diaphragm motion and deformation by at least two independent parameters.

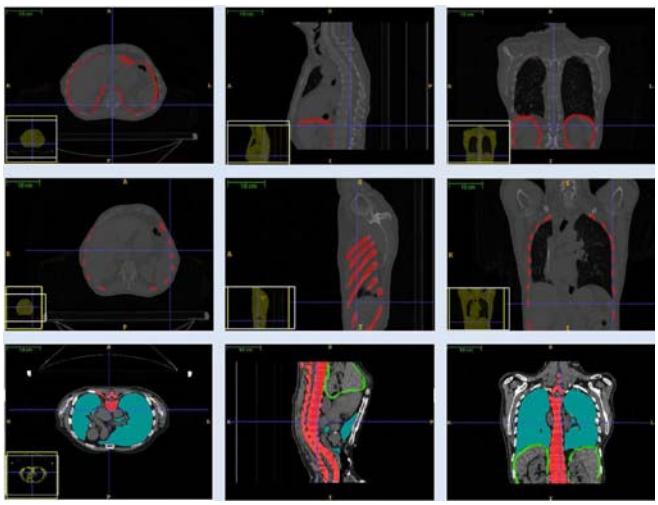

Fig. 3. Automatic and semi-automatic segmentation of the respiratory system: Ribs, human diaphragm and lungs.

II. Materials and methods

In order to build a geometrical model, we have used a 4D CT scan data covering the whole thorax of a patient. Consisting a set of 3 D CT scans at different respiratory states (full exhalation, intermediate stage and full inhalation). The CT images voxel size is $1.17 \times 1.17 \times 3$ mm^3 with $512 \times 512 \times 130$ voxels respectively in the left-right (X), dorsoventral (Y) and craniocaudal (Z) directions.

A. 3D Automatic and semi automatic segmentation

The diaphragm is a thin tissue, where the thickness is less than 2*mm*. In this work, the human diaphragm was segmented semi automatically using the snake evolution methodology available within ITK-SNAP library [1] (Fig.4). The diaphragm muscles and tendon cannot be identified separately on the CT images, neither visually nor automatically. However, according to [15], the mean central tendon surface area is 143 cm^2. This area does not vary to a large degree between one person and another. The thorax with musculoskeletal structure is segmented automatically based on our developed segmentation algorithms.

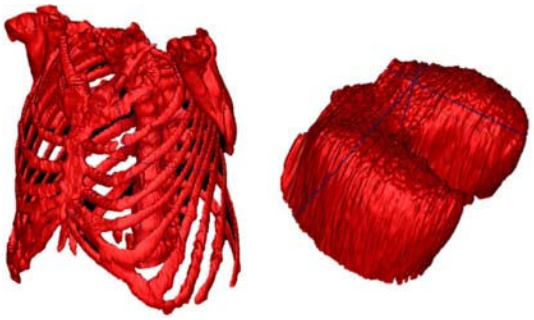

Fig. 4. 3D geometrical models issued directly from segmentation: human diaphragm and thorax .

B. 3D reconstruction

After segmentation, a 3D triangular surface mesh was created, using the marching cube algorithm (Fig.3). Due to the excessive number of nodes and large number of bad quality elements in initial meshes, which are common features in mesh based models, the different meshes are first smoothed, then decimated and smoothed again to remove decimation artefact. These oprations are achieved without reducing the mesh surface details. The obtained volumetric meshes, suitable for stress analysis are meshed with three dimensional (3D) first order tetrahedral element, were then input into finite element Abaqus solver [2].

III. Biomechanics and kinematics Modeling

From a biomechanical point of view, the respiratory system is an extremely complicated structure (Fig.5). In this section, we present an appropriate personalized biomechanical model of the respiratory system (diaphragm and thorax) and ribcage kinematics model based on finite helical axis method, where :

1) The diaphragm considered as a compressible heterogeneous solid with a linear elastic, the muscles in its peripheral part converging to a central tendon. The muscles of the diaphragm are of skeletal muscle type, and their action has the effect of shortening or lengthening of the muscles along their fiber direction.
2) The complete thorax behavior with musculoskeletal structure modeled as incompressible solid with an elastic linear behavior

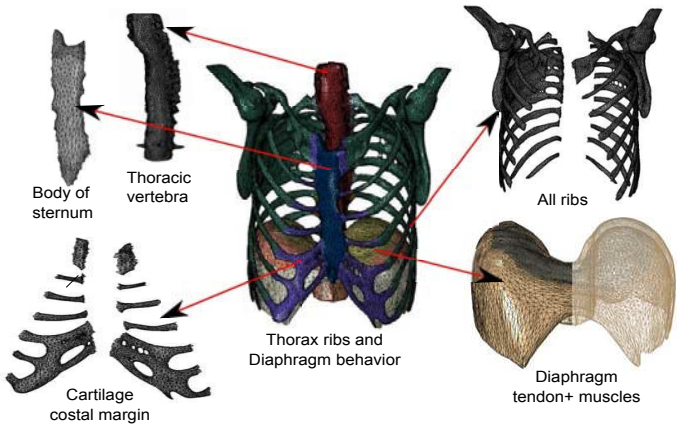

Fig. 5. Different part of the diaphragm and thorax: tendon, muscles tissues, ribs, thoracic vertebra, cartilage costal margin, Body of sternum.

A. Linear finite element formulation

Finite element simulations are performed using an industrial finite element software Abaqus.
For an isotropic elastic or hyperelastic material the elastic energy, noted W, can be written as:

$$W(\underline{\mathbf{E}}) = \frac{\lambda}{2}(tr\underline{\mathbf{E}})^2 + \mu\,(tr\underline{\mathbf{E}}^2) \tag{1}$$

where $\underline{\mathbf{E}}$ is the Green-Lagrange strain tensor, λ and μ are the Lame's coefficients.

$$\underline{\mathbf{E}} = \tfrac{1}{2}\left(\mathbf{grad}\,\underline{U} + \mathbf{grad}^T\,\underline{U} + \mathbf{grad}^T\,\underline{U}\,.\,\mathbf{grad}\,\underline{U}\right) \tag{2}$$

For small deformations, the Green-Lagrange strain tensor is linearized into the infinitesimal strain tensor:

$$\boldsymbol{\varepsilon} = \frac{1}{2}(\mathbf{grad}\,\underline{U} + \mathbf{grad}^T\,\underline{U}) \tag{3}$$

A displacement vector $\underline{U}$ based on finite element solution is obtained with the use the principal of virtual works.
The relation between the stress tensor and the strain tensor (Hooke's law), for isotropic material and for linear deformation, can be written as:

$$\varepsilon = \frac{1+\nu}{E}\sigma - \frac{\nu}{E}tr(\sigma)Id \tag{4}$$

[1]Free interactive software application that allows users to navigate three-dimensional medical images, manually delineate anatomical regions of interest, and perform automatic image segmentation

[2]The FE code Abaqus is developed by SIMULIA

E: Young's modulus and ν: Poisson's coefficient.
Other expression can be written, introduce Lame's constants, where μ:shearing coefficient, λ: compression coefficient.

$$\mu = \frac{E}{2(1+\nu)} \qquad \lambda = \nu\frac{E}{(1-2\nu)(1+\nu)} \tag{5}$$

The relation between the Cauchy stress tensor and the linearized strain tensor is written with Lame's coefficient in condensed vector notation as :

$$\left\{\boldsymbol{\sigma}\right\} = \lambda\left(tr\left\{\boldsymbol{\varepsilon}\right\}\right)\left[\mathbf{I}\right] + 2\mu\left\{\boldsymbol{\varepsilon}\right\} \tag{6}$$

where $\left[\mathbf{I}\right]$ is the identity matrix.
The principle of virtual work applied to a single tetrahedron T^{τ} leads to the elementary stiffness matrix $\left[\mathbf{K}^{\tau}\right]$ such that the elementary nodal force vector acting on a tetrahedron :

$$\left\{\mathbf{f}^{\tau}\right\} = \left[\mathbf{K}^{\tau}\right]\left\{\mathbf{u}^{\tau}\right\} \tag{7}$$

The Cauchy stress tensor σ_{ij} represents internal forces acting at a material point per unit area of the deformed solid.

B. Rib cage and intercostal muscles: Rib kinematics

Several authors have investigated the ribs kinematics. In [17], human rib displacements were studied and the transformation parameters where defined using planes attached to the ribs. Yet, several points on the two rib extremities could not be located in the same plane as the rib itself, Thus, those points were ignored.
A state of the art methodology to study human rib displacements using the finite helical axis method is presented in our last work [18]. Since ribs can be considered as rigid bodies in comparison with other surrounding anatomical elements, each rib transformation parameter is computed automatically between the initial and final states. The Fig.6 shows the principale of the

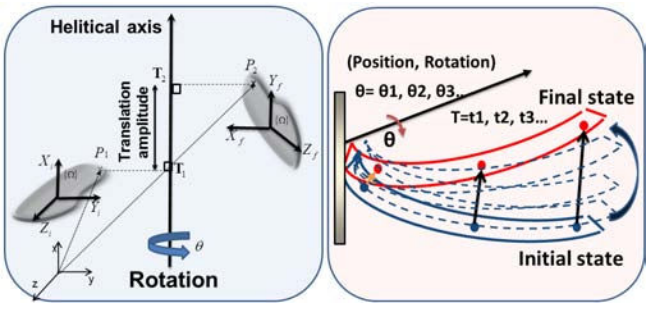

Fig. 6. Finite Helical Axis Method (FHAM) .

Finite Helical Axis Method (FHAM), where $P_1(X_i, Y_i, Z_i)$ is a coordinate system linked to a solid at an initial state and $P_2(X_f, Y_f, Z_f)$ is the same coordinate system after transformation:

$$\overrightarrow{P_1P_2} = 2\overrightarrow{k}\frac{tan\theta}{2} \times \left(\frac{\overrightarrow{T_1P_1} + \overrightarrow{T_2P_2}}{2}\right) + \overrightarrow{T_1T_2} \tag{8}$$

Rib positions can then be computed by interpolation at any intermediate state.

$$\left[\mathbf{P}\right]_{ij} = \begin{bmatrix} \alpha + kx^2\beta & kxky\alpha + kz\gamma & ky\gamma + kxkz\beta \\ kz\gamma + kxky\beta & \alpha + ky^2\beta & -kx\gamma + kykz\beta \\ -ky\gamma + kxkz\beta & kx\gamma + kykz\beta & \alpha + kz^2\beta \end{bmatrix} \tag{9}$$

with $\alpha = cos(\theta)$, $\beta = 1 - cos(\theta)$, $\gamma = sin(\theta)$.

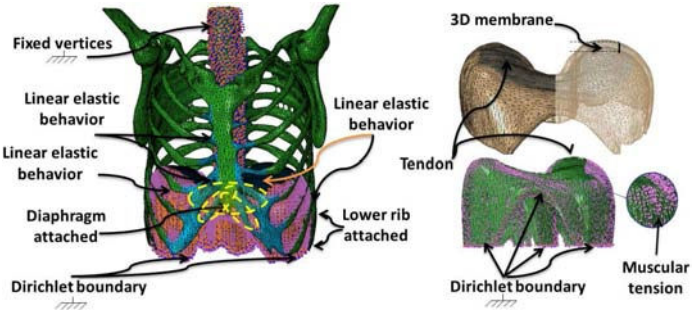

Fig. 7. The boundary conditions applied to the mesh nodes of the respiratory system: Human diaphragm and thorax.

C. Boundary condition

The boundary conditions are inferred from the anatomy and identified by medical experts (see Fig.7). The diaphragm is composed of two parts: 1) the tendon where the lungs and the heart lie, and 2) the muscle part that contracts and relaxes. The peripheral part, which consists of muscles, is linked to the lower thoracic cavity perimeter and has three major insertions: lumbar, sternum and ribs. The lumbar part is fixed to the lumbar vertebrae by means of the crura. The sternal part is attached to the internal surface of the xyphoid process. The costal part is attached to the internal surfaces of the lower six costal cartilages or ribs. The Dirichlet boundary condition are applied in lower part of the diaphragm. Two parameters are set to monitor diaphragm motion: the amplitude of muscle tension and ribs displacement.
The pressure is applied on the muscular part of the diaphragm. Rib displacement is coupled using an automatic rigid transformation by applying rotations and translations [18]. The surface tension models generate forces that only depends on its amplitude applied on the surface on the surface. When applying the tension $\overrightarrow{t_s}$ on the diaphragm muscles, the resulting force can be written as:

$$\overrightarrow{f} = \int_S \overrightarrow{t_s}\, dS = \alpha \int_S \overrightarrow{dir_s}\, dS \tag{10}$$

with S, α and $\overrightarrow{dir_s}$ respectively the mesh surface, the force amplitude and direction. The Fig.7 presents the radial direction of muscle forces, which corresponds anatomically to the direction of muscle fibers [14].

IV. Experiments and Validation

In order to demonstrate the validity of our biomechanical and kinematic model, a quantitative and qualitative analysis of simulations have been conducted. We have compared the

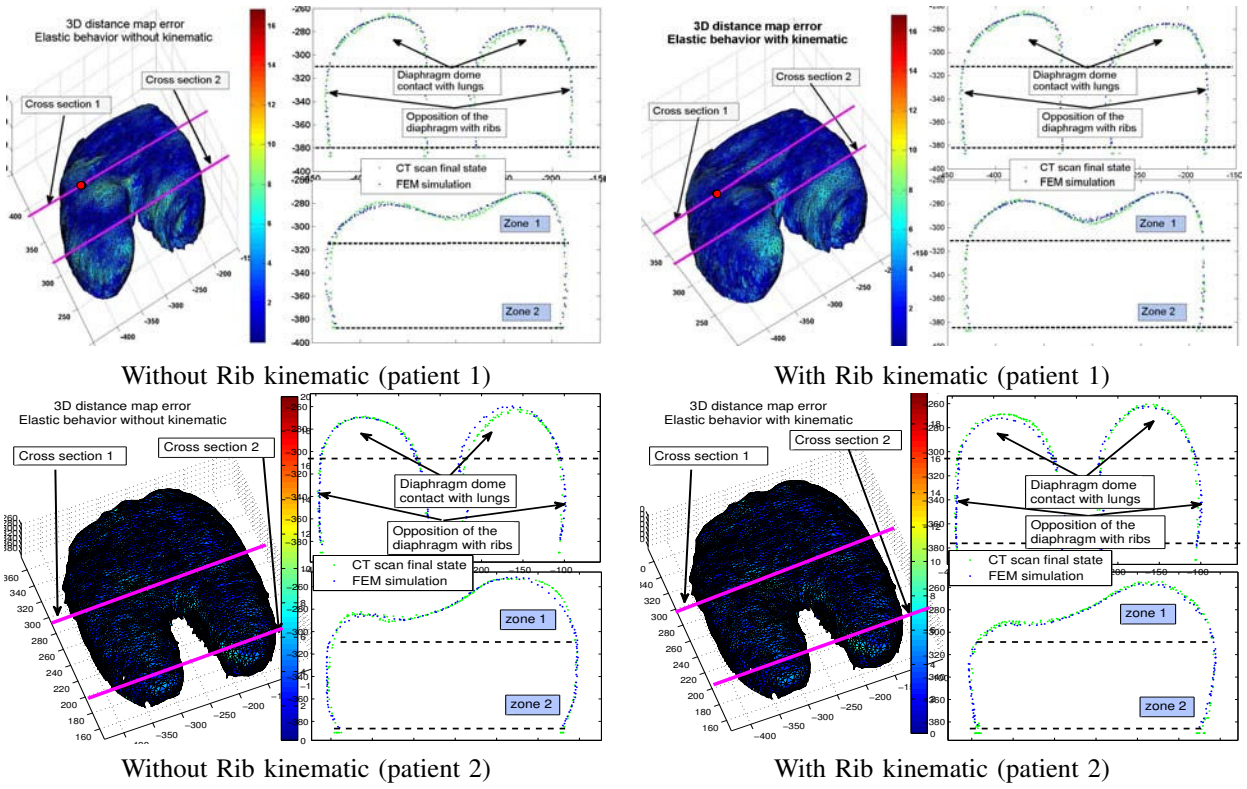

Fig. 8. 3D distance map error between the FE simulation and the reference real mesh at inspiration including or no rib kinematics. Color coding ranges from 0.0*mm* (blue) to 16.0*mm* (red), the vertical slices (showing the view from the cross sections) between the reference mesh and FE at expiration. Zone 1 presents the cross sections of interest region (contact with lungs). Zone 2 presents the peripheral contact between the diaphragm and ribcage.

TABLE I

COMPARAISON AND ERROR CALCULATION BETWEEN THE FEM SIMULATED MESHES VERSUS CLINICAL DATA: APPLIED TO 2 SCENARIOS, LINEAR ELASTIC BEHAVIOR WITH AND WITHOUT RIB KINEMATIC (RK), ε AVERAGE SURFACE ERROR AND *SD* STANDARD DEVIATION

	3D compare analysis											
	Patient 1						**Patient 2**					
	With RK			**Without RK**			**With RK**			**Without RK**		
Average distance (mm)	$\varepsilon_{positive}$	$\varepsilon_{negative}$	**SD**	$\varepsilon_{positive}$	$\varepsilon_{negative}$	**SD**	$\varepsilon_{positive}$	$\varepsilon_{negative}$	**SD**	$\varepsilon_{positive}$	$\varepsilon_{negative}$	**SD**
Whole Diaph	2.2	-1.43	2.3	2.4	-1.55	2.5	2.05	-1.67	2.26	2.28	-1.97	2.55
diaphragm/lungs contact (Zone 1)	1.49	-1.20	1.848	1.57	-1.415	1.91	1.83	-1.85	2.35	2.05	-1.96	2.46

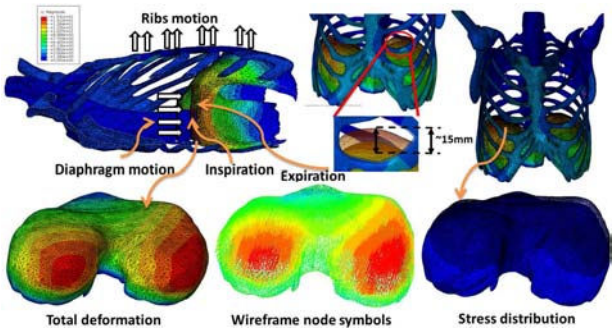

Fig. 9. FE simulation of the human respiratory system: stress distribution and the total deformation of the diaphragm including the thorax behavior.

TABLE II

MECHANICAL AND GEOMETRICAL PROPERTIES OF THE HUMAN DIAPHRAGM AND THORAX, WHERE E: YOUNG'S MODULUS, ρ: DENSITY AND ν: POISSON'S COEFFICIENT [14],[16] .

	Tendon	**Muscles**	**Ribs**	**Cartilage**	**Sternum**
E (MPa)	33	5.32	5000	49	11500
ν	0.33	0.33	0.3	0.4	0.3
ρ **(kg/m3)**	-	-	2000	1000	2000
Vertices	7138	9 691	46 235	6227	1877
Tetra	31 303	34 865	172 873	21533	6696

results of a simulated motion with the experimental data provided by the CT scan images. The mechanical and geometrical properties used in our finite element simulations are given in Table.II. First, we have investigated stress distribution and the total deformation of the diaphragm (Fig.9) during normal breathing between the initial state (inspiration) and the final state (expiration). We have observed the maximum displacement of the diaphragm inside the thorax on the right-posterior (RP) and left-posterior (LP) sides, also we notice a

slightly larger (RP) side motion than the (LP) side motion. This corresponds to the anatomical reality.

Then, we were interested in evaluating the impact of rib kinematic. We considered two scenarios: $\mathbf{S_1}$ and $\mathbf{S_2}$ whre the diaphragm and thorax are considered as compressible, heterogenous with a linear elastic behavior considering or not the effect of rib kinematics.

To evaluate quantitatively the distance between the mesh issued from CT scan images (original mesh) and the FEM displacement in computed. We computed for each organ the average distance between a FEM mesh vertex and its closest neighbour in the original mesh. The Fig.8 presents a 3D distance map and distance between cross sections measured on the original mesh and the FEM simulation mesh of the diaphragm at inspiration. The simulation shows that the developed finite element model is in a good agreement with the experimental data.

To improve the precision of our biomechanical simulation, a 3D comparaison (average shortest distance and volume difference) have been done between the FEM and CT images meshes. Table.I shows the average surface error of the whole of diaphragm and in the region of interest diaphragm/lungs contact zone. The color coding ranges correspond to the localized error. The range varies from blue 0*mm* error to red for the maximum error. We can state clearly that the behavior of the diaphragm is in good agreement with the CT scan images, and the role of rib kinematics. The average surface error is below 2*mm* in the region on interest corresponding to diaphragm/lungs contact zone. These errors depend mainly on the quality of the 3D segmentation algorithms, 3D geometrical reconstruction and the image resolution.

V. CONCLUSIONS

We have developed an accurate patient-specific finite element(FE) based biomechanical model in order to predict diaphragm deformation including the ribs kinematic. The simulation procedure involves a realistic behavior of the respiratory system. We first investigated the challenging issues in biomechanical modeling of the human diaphragm and ribs kinematic. The first results of our simulations are quite realistic, compared to the CT scan images. We can clearly see that the proposed physically-based FE model coupled with the rib kinematics is able to simulate correctly the diaphragm deformation including the real boundary conditions of the organs.

Currently, we are working on augmented reality system for patient-specific in real time integrating the diaphragm model in global biomechanical model of the respiratory system including lungs, pleura and soft tissues for different patients. Furthermore, these simulations should be correlated and controlled by external non-invasive surrogates. The other goal of this project is to generate and create a virtual 4D CT-scan image based virtual biomechanical model of the respiratory system. The objective of this study is to develop a new tool therapeutic to generate a 4D physical dose map needed for treatment planning systems.

REFERENCES

[1] K. L. Wu, G. L. Jiang, Y. Liao, H. Qian, L. J. Wang, X. L. Fu, S. Zhao, "Threedimensional conformal radiation therapy for non-small-cell lung cancer: A Phase I/II dose escalation clinical trial", Int. J. Rad. Oncol. Biol. Phys., vol. 57, issue 5, pp. 1336-1344, 2003.

[2] S. Sura, V. Gupta, E. Yorke, A. Jackson, H. Amols, K. E. Rosenzweig, "Intensitymodulated radiation therapy (IMRT) for inoperable non-small cell lung cancer: the Memorial Sloan-Kettering Cancer Center (MSKCC) experience", Radiother. Oncol. vol. 87, issue 1, pp. 17-23, 2008.

[3] A. Myronenko and X. Song, "Point-Set Registration: Coherent Point Drift," IEEE Trans. Pattern Analysis and Machine Intelligence, vol. 32, no. 12, 2010, pp. 2262-2275.

[4] M. Hiraoka, Y. Matsuo, K. Takayama, "Stereotactic Body Radiation Therapy for Lung Cancer: Achievements and Perspectives", Jpn. J. Clin. Oncol., vol. 40, issue 9, pp. 846-854, 2010.

[5] H. Nakayama, S. Sugahara, M. Tokita, H. Satoh, K. Tsuboi, S. Ishikawa, K. Tokuuye, "Proton beam therapy for patients with medically inoperable stage I non-small-cell lung cancer at the university of tsukuba", Int. J. Radiat. Oncol. Biol. Phys., vol. 78, issue 2, pp. 467-471, 2010.

[6] H. Shirato et al, Speed and amplitude of lung tumor motion precisely detected in four-dimensional setup and in real-time tumor-tracking radiotherapy. Int. J.Radia Oncolog Biol. Phys. 64(4): 1229-1236, 2006.

[7] D. Lee, A. Krupa. Intensity-based visual servoing for non-rigid motion compensation of soft tissue structures due to physiological motion using 4D ultrasound. In IEEE/RSJ Int. Conf. on Intelligent Robots and Systems, IROS'11, Pages 2831-2836, San Francisco, USA, 2011.

[8] A. Hostettler et al, Bulk modulus and volume variation measurement of the liver and the kidneys in vivo using abdominal kinetics during free breathing, in CMPB. Nov, 100(2):149-57, 2010.

[9] F. Vidal, P.F. Villard, E. Lutton, 'Tuning of patient specific deformable models using an adaptive evolutionary optimization strategy' IEEE TBME, Vol 59 (10), pp. 2942 - 2949, 2012.

[10] B. Fuerst et al. A personalized biomechanical model for respiratory motion prediction. MICCAI, 15(3):566-73. 2012.

[11] E. Promayon, P. Baconnier, A 3D discrete model of the diaphragm and human trunk, in 'ESAIM: Proceedings', pp. 66-77, 2008.

[12] P.F. Villard, W. Bourne, F. Bello, Interactive simulation of diaphragm motion through muscle and rib kinematics, 'Recent Advances in the 3D Physiological Human', Springer London, pp. 91-103, 2009.

[13] M. Behr, J. Prs, M. Lari, Y. Godio, Y. Jammes, C. Brunet, 'A three-dimensional human trunk model for the analysis of respiratory mechanics', Journal of biomechanical engineering 132, 014501-1-014501-4, 2010.

[14] M. Pato, N. Santos, P. Areias, E. Pires, M. de Carvalho, S.Pinto, D. Lopes, 'Finite element studies of the mechanical behaviour of the diaphragm in normal and pathological cases', CMBBE 14(6), 505-513, 2011.

[15] P. Cluzel, T. Similovsky, C.C Lefebvre, M. Zelter, J.P. Derenne, P. Grenier, 'Diaphragm and chest wall: Assessment of the inspiratory pump with MR imaging Preliminary observations', Radiology 215, 574-583, 2000.

[16] H. Kimpara et al, Development of a Three-Dimensional Finite Element Chest Model for the 5(th) Percentile Female, Stapp Car Crash J.Nov;49:251-69, 2005.

[17] T. Wilson et al, Respiratory effects of the external and internal intercostal muscles in humans, J of Phys, 503(2), 319-330, 2001.

[18] A.L. Didier, P.F. Villard, J.Saade, J.M. Moreau, M. Beuve, B. Shariat, A chest wall model based on rib kinematics, in international conference in visualization', IEEE computer society, pp. 159-164, 2009.

[19] J. Saade, D.A-L Didier, P.F. Villard, R. Buttin, JM. Moreau, M. Beuve, B. Shariat,'A Preliminary Study For A Biomechanical Model Of The Respiratory System'. Engineering and Computational Sciences for Medical Imaging in Oncology - VISAPP, Angers, France. pp. 509-515. ISBN 978-989-674-028-3, 2010.

[20] H. Ladjal, J. Saade, M. Beuve, J. Azencot, JM. Moreau, B. Shariat, '3D biomechanical modeling of the diaphragm', World Congress on Medical Physics and Biomedical Engineering, IFMBE Proceedings vol. 39. pp. 2188-2191. ISBN 978-3-642-29305-4, 2012.